A DECOMPOSITION METHOD FOR THE ELECTROMAGNETIC SCATTERING FROM A CONDUCTIVE OBJECT BURIED IN A LOSSY MEDIUM

S. Makal and A. Kizilay

Department of Electronics and Communications Engineering
Yildiz Technical University, Istanbul, 34349, Turkey
smakal@yildiz.edu.tr, akizilay@yildiz.edu.tr

Abstract ─ A new numerical solution method is presented for the electromagnetic field scattered by a perfectly conducting (PEC) cylindrical object with an arbitrary cross-section buried in a lossy dielectric half-space. The dielectric half-space is considered to be flat, and the method is outlined for TM_z (horizontally) polarized incident wave. The surface equivalence principle and a decomposition method are utilized to form a set of electric field integral equations (EFIEs) for the currents on the object and the portion of the surface most strongly interacting with the object. To obtain the scattered electric field, the EFIEs are solved in the frequency domain using the method of moments (MoM).

Index Terms ─ Electromagnetic scattering, integral equations, method of moments, perturbational field.

I. INTRODUCTION

Solution of the electromagnetic scattering by buried objects has been the interest of many researches. Therefore, several techniques have been employed to obtain the scattered fields. This is because scattered field values can be used in nondestructive evaluation applications such as detecting landmines, buried pipes, near-surface geophysical exploration, and also archeological studies [1-6]. As a result, an efficient way of calculating scattered field is important for ground-penetrating radar applications.

Previously, the problem for a cylinder buried in a medium having a flat surface has been studied by many researches. For example, Uzunoglu et al.

have computed the scattered electric field from underground tunnels using a Green's function approach, and analyzed the scattered amplitude for various observation angles [7]. Kanellopoulos et al. have used the same analytical approach for conducting wires buried in earth [8]. Also, "B" approximation and Sommerfield integrals with fast evaluation methods have been the other ways to build an analytical solution for buried scatterer [9-11]. Naqvi et al. have used plane wave expansion and excitation of current on a cylinder for the scattered electric field from a conducting cylinder deeply buried in a dielectric half-space [12]. Another analytical method containing plane wave representation has been developed by Ahmed et al. [13].

In this paper, the scattered electric field from a PEC cylindrical object of arbitrary cross-section buried in a lossy half-space is computed by a new numerical solution method. The basis of the new solution method is that if an object is close to the surface, the electromagnetic fields will be nearly identical to that without the object, except within the region of finite extent near the object [14, 15]. Thus, the equivalent current on the surface will be affected only in a finite portion of the surface near the object. By using this assumption, the EFIEs for the induced current on the PEC object and the perturbation current (the difference current with object present and with object absent) on the surface are obtained. Then, the EFIEs are solved by MoM in frequency domain.

II. THEORY

The geometry of the problem is shown in

Fig.1. A TM_z plane wave $\vec{E}^i$ is assumed to be incident on a cylindrical object of arbitrary cross-section buried in a two-dimensional infinite flat surface with the incidence angle of ϕ_i:

$$\vec{E}^i(x,y) = \hat{z}\, E_0\, e^{jk_0(x\cos\phi_i + y\sin\phi_i)}, \qquad (1)$$

where $k_0 = \omega\sqrt{\mu_0\varepsilon_0}$. A PEC object is located h_c below the surface. The distance between y-axis and the object axis is indicated by x_c. The flat surface is represented by S_d, and $\hat{n}_d$ is the outward unit normal vector to S_d. The object surface is represented by S_c, and $\hat{n}_c$ is the outward unit normal vector to S_c.
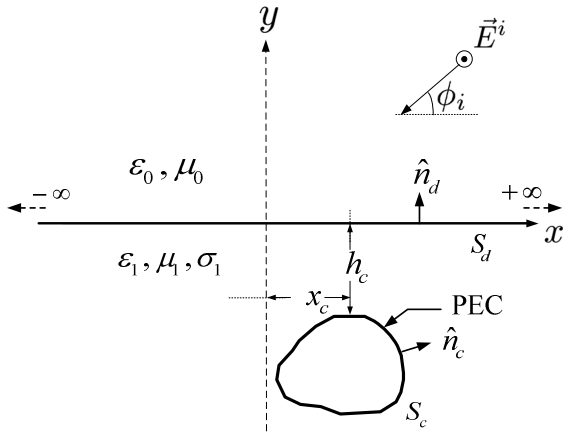

Fig. 1. The geometry of the problem.

The scattered electric field ($\vec{E}^s$) can be written as the sum of the scattered field from the PEC object and the flat surface:

$$\vec{E}^s = \vec{E}^S + \vec{E}^T. \qquad (2)$$

S and T indicate surface and object, respectively. The scattered electric field from the surface can be written as;

$$\vec{E}^S = \vec{E}^I + \vec{E}^P, \qquad (3)$$

where $\vec{E}^P$ is the perturbational field produced by the difference, or perturbation currents $\vec{J}_d^p$ and $\vec{M}_d^p$, and $\vec{E}^I$ is the field due to currents $\vec{J}^I$ and $\vec{M}^I$ on the surface which is impressed by the incident field without the object present. Therefore, the difference currents can be defined as $\vec{J}_d^p = \vec{J}^S - \vec{J}^I$ and $\vec{M}_d^p = \vec{M}^S - \vec{M}^I$. Here, $\vec{J}^S$

and $\vec{M}^S$ represent the equivalent currents on the surface. Then, substituting equation (3) into the equation (2) gives,

$$\vec{E}^s = \vec{E}^I + \vec{E}^P + \vec{E}^T. \qquad (4)$$

The unknown currents are the equivalent perturbation currents on the surface and the induced current on the object. These currents can be obtained by using the surface equivalence principle that is well-known in literature [16]. This principle has been used and explained by many researches [17, 20].

Before applying the surface equivalence principle to the original problem, the scattered electric field $\vec{E}^I$ should be obtained when the flat surface is the only scatterer. Thus, the flat surface is chosen to be the only scatterer shown in Fig. 2.
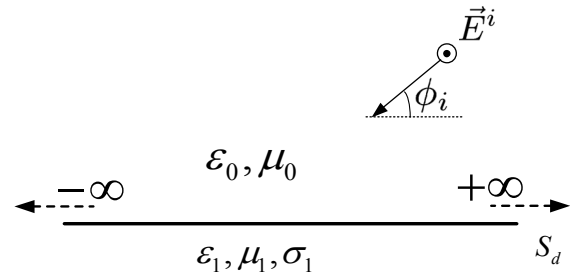

Fig. 2. The flat surface as a scatterer.

Figure 3 shows the external equivalence principle applied to the problem in Fig. 2. The whole space parameters are chosen as (ε_0, μ_0) [19, 20]. The surface is replaced by surface electric $(\vec{J}^I)$ and magnetic $(\vec{M}^I)$ currents. At any point outside the surface, the total fields are $\vec{E}$ and $\vec{H}$. The total fields are zero under the surface;

$$\vec{E}^i + \vec{E}_{ext}^I = 0 \Rightarrow S_d^-, \qquad (5)$$

$$\vec{H}^i + \vec{H}_{ext}^I = 0 \Rightarrow S_d^-. \qquad (6)$$

Here, *ext* means external and S_d^- represents the surface just inside S_d.

Then, the internal equivalence principle is applied in Fig. 4 to the problem shown in Fig. 2. Therefore, the whole space parameters are chosen as $(\varepsilon_1, \mu_1, \sigma_1)$ [19, 20]. The surface is replaced by surface electric $(-\vec{J}^I)$ and magnetic $(-\vec{M}^I)$ currents.
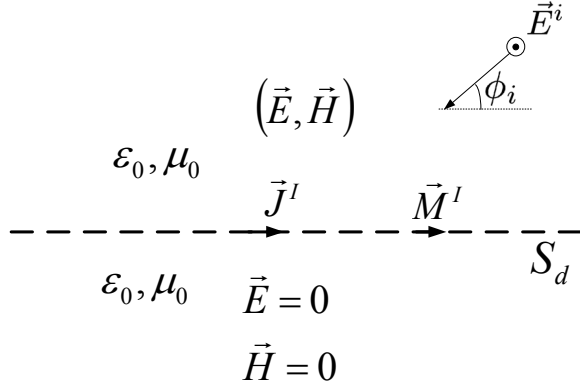
Fig. 3. External equivalence applied to the problem in Fig. 2.

The total fields are zero at any point external to S_d;

$$\vec{E}^I_{int} = 0 \Rightarrow S_d^+, \tag{7}$$

$$\vec{H}^I_{int} = 0 \Rightarrow S_d^+. \tag{8}$$

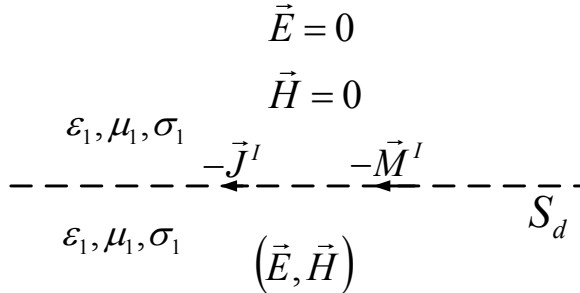Here, *int* means internal, and S_d^+ represents the surface just outside S_d.

Fig. 4. Internal equivalence applied to the problem in Fig. 2.

Now, with the knowledge of scattered electric fields on the surface when there is not any object, the original problem in Fig. 1 can be solved. Initially, the external equivalence principle is applied in Fig. 5.

The total field outside the surface is the sum of the incident, and scattered field;

$$\vec{E} = \vec{E}^i + \vec{E}^s, \tag{9}$$

$$\vec{H} = \vec{H}^i + \vec{H}^s, \tag{10}$$

and the scattered electric field is;

$$\vec{E}^s = \vec{E}^I_{ext} + \vec{E}^P_{ext}. \tag{11}$$

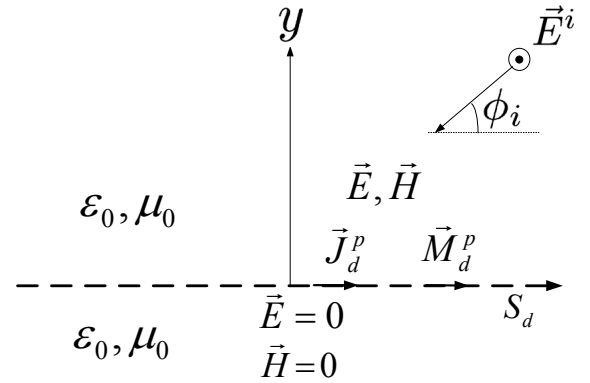In Fig. 5, $\vec{J}_d^p$ and $\vec{M}_d^p$ are the perturbation currents;

Fig. 5. The external equivalence principle applied to the problem in Fig. 1.

$$\vec{J}_d^p = \hat{n}_d \times \vec{H}(S_d^+), \tag{12}$$

$$\vec{M}_d^p = \vec{E}(S_d^+) \times \hat{n}_d. \tag{13}$$

The total field is zero just inside the surface S_d;

$$\vec{E}^s = -\vec{E}^i \Rightarrow S_d^-. \tag{14}$$

Then, the field caused by perturbation currents becomes;

$$\vec{E}^P_{ext} = -\vec{E}^I_{ext} - \vec{E}^i \Rightarrow S_d^-. \tag{15}$$

Now, equation (5) is used in equation (15), then the value of the perturbation field on S_d^- becomes,

$$\vec{E}^P_{ext}\left(\vec{J}_d^p, \vec{M}_d^p\right) = 0 \Rightarrow S_d^-. \tag{16}$$

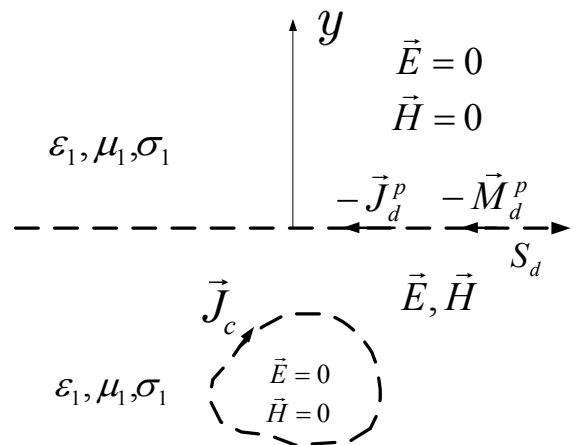Then, the internal equivalence principle is applied in Fig. 6 to the problem shown in Fig. 1.

Fig. 6. The internal equivalence principle applied to the problem in Fig. 1.

There is no incident wave, and the total fields under the surface contain just the scattered fields;

$$\vec{E} = \vec{E}^s, \tag{17}$$

$$\vec{H} = \vec{H}^s. \tag{18}$$

The scattered electric field is expressed;

$$\vec{E}^s = \vec{E}^I_{int} + \vec{E}^P_{int} + \vec{E}^T \tag{19}$$

The total electric field is zero outside S_d :

$$\vec{E}^P_{int}\left(-\vec{J}^p_d, -\vec{M}^p_d\right) + \vec{E}^T\left(\vec{J}_c\right) = -\vec{E}^I_{int} \Rightarrow S^+_d. \tag{20}$$

After equation (7) is used in equation (20), the scattered electric field on S^+_d becomes,

$$\vec{E}^P_{int}\left(-\vec{J}^p_d, -\vec{M}^p_d\right) + \vec{E}^T\left(\vec{J}_c\right) = 0 \Rightarrow S^+_d. \tag{21}$$

The total field is also zero inside S_c ,

$$\vec{E}^P_{int}\left(-\vec{J}^p_d, -\vec{M}^p_d\right) + \vec{E}^T\left(\vec{J}_c\right) = -\vec{E}^I_{int} \Rightarrow S^-_c, \tag{22}$$

where S^-_c represents the surface just inside S_c and $\vec{J}_c$ is the equivalent current on the object;

$$\vec{J}_c = \hat{n}_c \times \vec{H}(S^+_c). \tag{23}$$

$\vec{E}^I_{int}$ on S^-_c is the electric field value on the object points when the object is absent. Therefore, this electric field can be obtained analytically in a closed form as;

$$\vec{E}^I_{int} = \hat{z}\, T\, E_0 e^{jk_1(x\sin\phi_t + y\cos\phi_t)}. \tag{24}$$

Here, $k_1 = \omega\sqrt{\mu_1 \varepsilon_c}$ and $\varepsilon_c = \varepsilon_1\left(1 - j\dfrac{\sigma_1}{\omega\varepsilon_1}\right)$. The transmission coefficient indicated by T ;

$$T = \frac{2\eta_1 \cos\phi_i}{\eta_1 \cos\phi_i + \eta_0 \cos\phi_t}, \tag{25}$$

where $\eta_0 = \sqrt{\mu_0 / \epsilon_0}$ and $\eta_1 = \sqrt{\mu_1 / \epsilon_c}$ are the intrinsic impedance of free and lossy half-space, respectively. Here, ϕ_t is the transmission angle and defined by Snell's law;

$$\phi_t = \sin^{-1}\left(\sqrt{\frac{\varepsilon_0 \mu_0}{\varepsilon_c \mu_1}} \cos\phi_i\right). \tag{26}$$

In other words, there are three equations (16), (21), and (22) to be solved by using MoM and the three unknown currents to calculate the scattered field.

The electric field is expressed in terms of electric and magnetic potential functions [17], and

equations (16), (21), and (22) can be rewritten as;

$$-j\omega A^{ext}_z\left(\vec{J}^p_d\right) - \frac{1}{\varepsilon_0}\left[\nabla \times \vec{F}^{ext}\left(\vec{M}^p_d\right)\right]_z = 0,\ S^-_d, \tag{27}$$

$$-j\omega A^{int}_z\left(-\vec{J}^p_d\right) - j\omega A^{int}_z\left(\vec{J}_c\right)$$
$$-\frac{1}{\varepsilon_c}\left[\nabla \times \vec{F}^{int}\left(-\vec{M}^p_d\right)\right]_z = 0,\ S^+_d, \tag{28}$$

$$-j\omega A^{int}_z\left(-\vec{J}^p_d\right) - j\omega A^{int}_z\left(\vec{J}_c\right)$$
$$-\frac{1}{\varepsilon_c}\left[\nabla \times \vec{F}^{int}\left(-\vec{M}^p_d\right)\right]_z = -\left[\vec{E}^I_{int}\right]_z,\ S^-_c, \tag{29}$$

where $\vec{A}$ and $\vec{F}$ denote the magnetic and electric vector potential, respectively. They are given by the following line integrals:

$$\vec{A}(\vec{\rho}) = \frac{\mu}{4j}\int_{C_j} \vec{J}(\vec{\rho}')H^{(2)}_0\left(k|\vec{\rho} - \vec{\rho}'|\right)dl', \tag{30}$$

$$\vec{F}(\vec{\rho}) = \frac{\varepsilon}{4j}\int_{C_m} \vec{M}(\vec{\rho}')H^{(2)}_0\left(k|\vec{\rho} - \vec{\rho}'|\right) dl', \tag{31}$$

where $\vec{\rho}'$ represents the source points, and $\vec{\rho}$ is a two-dimensional position vector. The contours over $\vec{J}$ and $\vec{M}$ are C_j and C_m, respectively.

Three equations (27, 28, 29) are solved numerically using MoM for three unknown surface currents $(\vec{J}^p_d, \vec{M}^p_d, \vec{J}_c)$. The currents on the surfaces of S_d and S_c are approximated by linear segments:

$$\vec{J}_c(\vec{\rho}') = \hat{z}\sum_{i=1}^{N_c} I^c_i P^c_i(\vec{\rho}'), \tag{32}$$

$$\vec{J}^p_d(\vec{\rho}') = \hat{z}\sum_{i=1}^{N_d} I^d_i P^d_i(\vec{\rho}'), \tag{33}$$

$$\vec{M}^p_d(\vec{\rho}') = \sum_{i=1}^{N_d} \hat{\tau}_i K^d_i P^d_i(\vec{\rho}'), \tag{34}$$

where N_c and N_d are the numbers of segments on S_c and S_d, respectively. I^c_i and I^d_i are the unknown values of electric current on the ith segment of S_c and S_d, respectively. K^d_i denotes the value of the magnetic current on the ith segment of N_d. The unit vector in the

circumferential direction tangent to the ith segment of S_d is denoted by $\hat{\tau}_i$, and the unit vector in the z-direction is denoted by $\hat{z}$. Pulse functions (P^c, P^d) are chosen as the expansion functions.

Equations (27), (28), and (29) can be rewritten using equations (32), (33), and (34);

$$-\frac{\omega\mu_0}{4}\sum_{i=1}^{N_d}I_i^d\int_{C_{di}}H_0^{(2)}\left(k_0\left|\vec{\rho}-\vec{\rho}'\right|\right)dl'$$

$$-\frac{jk_0}{4}\sum_{i=1}^{N_d}K_i^d\int_{C_{di}}H_1^{(2)}\left(k_0\left|\vec{\rho}-\vec{\rho}'\right|\right) \quad (35)$$

$$\times\frac{\hat{n}_i^d\cdot\left(\vec{\rho}-\vec{\rho}'\right)}{\left|\vec{\rho}-\vec{\rho}'\right|}dl'=0, \quad S_d^-,$$

$$\frac{\omega\mu_1}{4}\sum_{i=1}^{N_d}I_i^d\int_{C_{di}}H_0^{(2)}\left(k_1\left|\vec{\rho}-\vec{\rho}'\right|\right)dl'$$

$$-\frac{\omega\mu_1}{4}\sum_{i=1}^{N_c}I_i^c\int_{C_{ci}}H_0^{(2)}\left(k_1\left|\vec{\rho}-\vec{\rho}'\right|\right)dl'$$

$$+\frac{jk_1}{4}\sum_{i=1}^{N_d}K_i^d\int_{C_{di}}H_1^{(2)}\left(k_1\left|\vec{\rho}-\vec{\rho}'\right|\right) \quad (36)$$

$$\times\frac{\hat{n}_i^d\cdot\left(\vec{\rho}-\vec{\rho}'\right)}{\left|\vec{\rho}-\vec{\rho}'\right|}dl'=0, \quad S_d^+,$$

$$\frac{\omega\mu_1}{4}\sum_{i=1}^{N_d}I_i^d\int_{C_{di}}H_0^{(2)}\left(k_1\left|\vec{\rho}-\vec{\rho}'\right|\right)dl'$$

$$-\frac{\omega\mu_1}{4}\sum_{i=1}^{N_c}I_i^c\int_{C_{ci}}H_0^{(2)}\left(k_1\left|\vec{\rho}-\vec{\rho}'\right|\right)dl'$$

$$+\frac{jk_1}{4}\sum_{i=1}^{N_d}K_i^d\int_{C_{di}}H_1^{(2)}\left(k_1\left|\vec{\rho}-\vec{\rho}'\right|\right) \quad (37)$$

$$\times\frac{\hat{n}_i^d\cdot\left(\vec{\rho}-\vec{\rho}'\right)}{\left|\vec{\rho}-\vec{\rho}'\right|}dl'=-E_{int}^I, \quad S_c^-,$$

where $H_0^{(2)}$ is the zeroth-order Hankel function of the second kind, $H_1^{(2)}$ is the first-order Hankel function of the second kind, C_d and C_c are the contours representing of S_d and S_c, respectively. Then, pulse weighting functions are used to transform these EFIEs to linear equations. These linear equations are solved to obtain the unknown

currents, and the far scattered field can be computed using only $\vec{J}_d^p$ and $\vec{M}_d^p$:

$$E_z^s = -\frac{\omega\mu_0}{4}\sqrt{\frac{2j}{k_0\pi}}\frac{e^{-jk_0\rho}}{\sqrt{\rho}}\sum_{i=1}^{N_d}I_i^d e^{-jk_0\left(x'\cos\phi_s+y'\sin\phi_s\right)}\Delta_i^d$$

$$+\frac{jk_0}{4}\sqrt{\frac{2j}{k_0\pi}}\frac{e^{-jk_0\rho}}{\sqrt{\rho}}\sum_{i=1}^{N_d}K_i^d e^{-jk_0\left(x'\cos\phi_s+y'\sin\phi_s\right)}\Delta_i^d,$$

$$(38)$$

where ϕ_s is the scattering angle, and Δ^d is the length of the segment on S_d.

III. NUMERICAL RESULTS

If it is not indicated otherwise; for all MoM solutions, the value of 20 points per free-space wavelength (λ_0) is used to represent the currents on the object and the surface. The object is chosen to be a PEC cylinder with circular cross-section of radius r_a (Fig. 7), and the perturbation currents' behaviors are investigated in Fig. 8 to validate the assumption that the equivalent current on the surface will be affected only in a finite portion of the surface near the object. As expected, when the object is buried deeper, the perturbation currents spread along the surface. So, it is important to select the truncation width (wl) carefully.
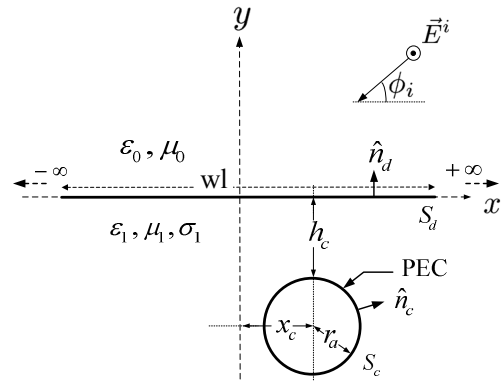

Fig. 7. The geometry used for the numerical results.

After establishing the validity of our assumption, it is also necessary to determine the accuracy of the method. This can be done by choosing the space parameters under the flat surface as (ε_0, μ_0). Thus, the scattered field is expected to behave like a PEC cylinder. The

scattered E-field is first solved by the decomposition method, and then by the analytical method [21]. Then, these two results are compared in Fig. 9. It is seen that if the truncation width is chosen to be sufficiently long, the decomposition method gives very accurate results.

The root-mean square error (E_{RMS}) between the decomposition method and the analytical solution is calculated by using;
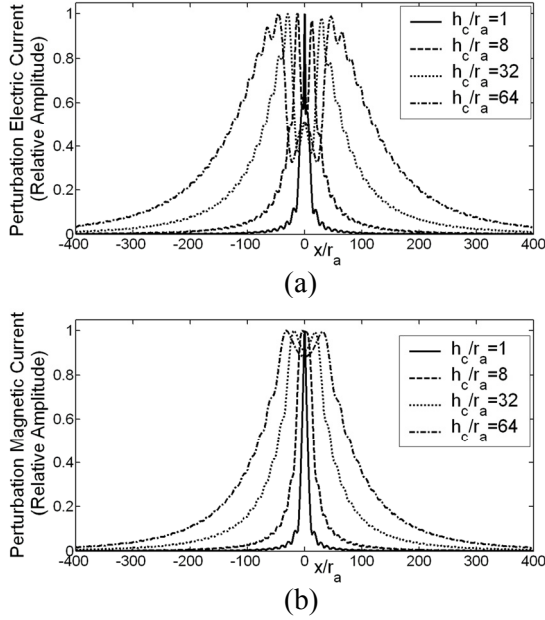

(a)

(b)

Fig. 8. Perturbation (a) electric and (b) magnetic currents on the flat surface for $f=1$ GHz, $\phi_i = 20°$, $r_a = 0.01$ m, $x_c / r_a = 0.0$, $\varepsilon_1 = 15 \varepsilon_0$ F/m, $\mu_1 = \mu_0$ H/m, and $\sigma_1 = 0.01$ Sm^{-1}.
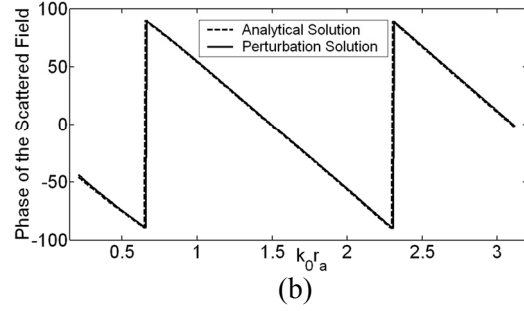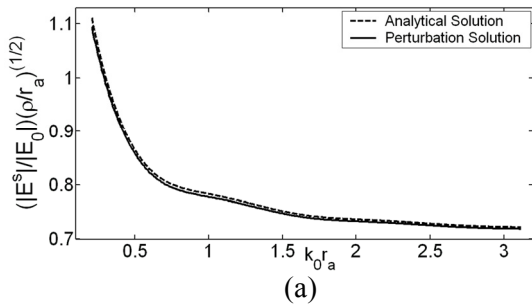

(a)

(b)

Fig. 9. Scattered field (a) normalized amplitude and (b) phase for $r_a = 0.01$ m, $\phi_i = 90°$, $h_c / r_a = 1.0$, $x_c / r_a = 0.0$, wl$/ r_a = 500$, $\varepsilon_1 = \varepsilon_0$ F/m, and $\mu_1 = \mu_0$ H/m.

$$E_{RMS}\left(\%\right) = \sqrt{\frac{\left|E^A - E^P\right|^2}{\left|E^A\right|^2}}, \qquad (39)$$

where E^A and E^P, show analytical and decomposition solutions, respectively. The number of points on the cylinder is chosen to be 50. Then, the RMS error is calculated and shown in Fig. 10. It is seen that $E_{RMS}(\%) \leq 0.227\, e^{-0.0033\,\mathrm{wl}/h_c}$, so the solution converges exponentially with respect to wl/h_c and the solution becomes more accurate for increasing truncation width.
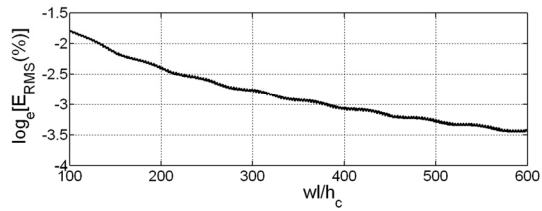

Fig. 10. The approximation difference for $r_a = 0.01$ m, $\phi_i = 90°$, $h_c / r_a = 1.0$, $x_c / r_a = 0.0$, $\varepsilon_1 = \varepsilon_0$ F/m, and $\mu_1 = \mu_0$ H/m.

To validate the decomposition method for lossy half-space, the solution is compared to the results in [8] including Green's function approach. The comparison is shown in Fig. 11. Increasing the truncation width makes the solution to converge the result of Green's function approach.
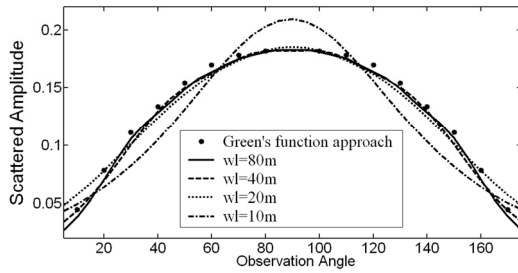
Fig. 11. Scattered amplitude from a cylindrical scatterer with circular cross-section for $r_a = 0.3$ m, $h_c = 1.7$ m, $x_c / r_a = 0.0$, $\varepsilon_1 = 15 \varepsilon_0$ F/m, $\mu_1 = \mu_0$ H/m, $\phi_i = 60°$, $f = 30$ MHz, and $\sigma_1 = 0.01$ Sm^{-1}.

After determining the method's accuracy, the object is chosen as a cylinder with elliptical cross-section in Fig. 12. The effect of the incident angle is noticeable on the scattered amplitude. There is a reduction of the magnitude of the scattered field as the incident angle deviates from $90°$. Also, the scattered energy is concentrated around a scattering angle of $90°$ even for a very small incident angle.
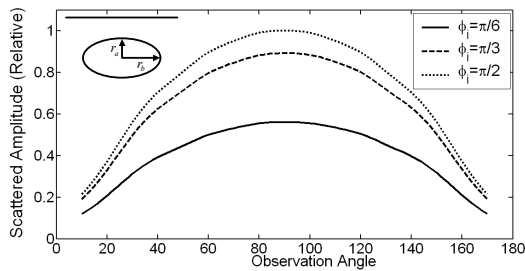

Fig. 12. Relative scattered amplitude from a cylindrical scatterer with elliptical cross-section for $r_a = 0.02$ m, $r_b = 0.01$ m, $h_c / r_b = 1.0$, $x_c / r_a = 0.0$, $\varepsilon_1 = 15 \varepsilon_0$ F/m, $\mu_1 = \mu_0$ H/m, and $\sigma_1 = 0.01$ Sm^{-1}.

IV. CONCLUSION

The scattered electric field from a conducting cylinder buried in a lossy medium having an infinite flat surface excited by a TM$_z$ polarized electromagnetic wave has been solved by a new numerical solution method. The validity of perturbation assumption is shown by calculating the perturbation currents on the flat surface. It is shown that the perturbation currents on the flat surface become negligible except within the region of finite extent near the object for lossy medium. Also, to investigate the accuracy of the method, the medium parameters are taken to be space parameters. It is seen that the method is very accurate. A detailed study of short-pulse scattering from objects buried in a lossy half-space will be undertaken in the future.

REFERENCES

[1] T. Dogaru, L. Carin, "Time-Domain Sensing of Targets Buried under a Rough Air-Ground Interface," *IEEE Transactions on Antennas and Propagation*, vol. 46, no. 3, pp. 360-372, 1998.

[2] Y. Altuncu, I. Akduman, and A. Yapar, "Detecting and Locating Dielectric Objects Buried under a Rough Interface," *IEEE Geoscience and Remote Sensing Letters*, vol. 4, no. 2, pp. 251-255, 2007.

[3] G. L. Plett, T. Doi, and D. Torrieri, "Mine Detection using Scattering Parameters," *IEEE Transactions on Neural Networks*, vol. 8, no. 6, pp. 1456-1467, 1997.

[4] W. Chien and C-C. Chiu, "Cubic-Spline Expansion with GA for Half-Space Inverse Problems," *Applied Computational Electromagnetic Society (ACES) Journal*, vol. 20, no. 2, pp. 136-143, 2005.

[5] C. Huang, C. Chen, C. Chiu, and C. Li, "Reconstruction of the Buried Homogenous Dielectric Cylinder by FDTD and Asynchronous Particle Swarm Optimization," *Applied Computational Electromagnetic Society (ACES) Journal*, vol. 25, no. 8, pp. 672-681, 2010.

[6] K. P. Prokopidis and T. D. Tsiboukis, "Modeling of Ground-Penetrating Radar for Detecting Buried Objects in Dispersive Soils," *Applied Computational Electromagnetic Society (ACES) Journal*, vol. 22, no. 2, pp. 287-294, 2007.

[7] N. K. Uzunoglu and J. D. Kanellopoulos, "Scattering From Underground Tunnels,"

Journal of Physics A: Mathematical and General, vol. 15, no. 2, pp. 459-471, 1982.

[8] J. D. Kanellopoulos and N. E. Buris, "Scattering From Conducting Cylinders Embedded in a Lossy Medium," *International Journal of Electronics*, vol. 57, no. 3, pp. 391-401, 1984.

[9] D. A. Hill, "Electromagnetic Scattering by Buried Objects of Low Contrast," *IEEE Transactions on Geoscience and Remote Sensing*, vol. 26, no. 2, pp. 195-203, 1988.

[10] T. J. Cui and W. C. Chew, "Efficient Evaluation of Sommerfeld Integrals for TM Wave Scattering by Buried Objects," *Journal of Electromagnetic Waves and Applications*, vol. 12, no. 5, pp. 607-657, 1998.

[11] T. J. Cui, W. C. Chew, and W. Hong, "New Approximate Formulations for EM Scattering by Dielectric Objects," *IEEE Transactions on Antennas and Propagation*, vol. 52, no. 3, pp. 684-692, 2004.

[12] Q. A. Naqvi, A. A. Rizvi, and Z. Yaqoob, "Scattering of Electromagnetic Waves from a Deeply Buried Circular Cylinder," *Progress in Electromagnetics Research*, vol. 27, pp. 37-59, 2000.

[13] S. Ahmed and Q. A. Naqvi, "Electromagnetic Scattering from a Perfect Electromagnetic Conductor Cylinder Buried in a Dielectric Half-Space," *Progress in Electromagnetics Research*, vol. 78, pp. 25-38, 2008.

[14] A. Kizilay, *A Perturbation Method for Transient Multipath Analysis of Electromagnetic Scattering from Objects above Periodic Surfaces*, Ph.D. Dissertion, Michigan State University, 2000.

[15] A. Kizilay and E. Rothwell, "Efficient Computation of Transient TM Scattering from a Cylinder above an Infinite Periodic Surface," *Journal of Electromagnetic Waves and Applications*, vol. 13, no. 7, pp. 943-961, 1999.

[16] R. F. Harrington, *Time Harmonic Electromagnetic Fields*, McGraw-Hill, New York, 1961.

[17] A. W. Glisson, "An Integral Equation for Electromagnetic Scattering from Homogeneous Dielectric Bodies," *IEEE Transactions on Antennas and Propagation*, vol. 32, no. 2, pp. 173-175, 1984.

[18] A. J. Booysen, "A Physical Interpretation of the Equivalence Theorem," *IEEE Transactions on Antennas and Propagation*, vol. 48, no. 8, pp. 1260-1262, 2000.

[19] E. Arvas, M. Ross, and Y. Qian, "TM Scattering from a Conducting Cylinder of Arbitrary Cross-Section Covered by Multiple Layers of Lossy Dielectrics," *IEE Proceedings H*, vol. 135, no. 4, pp. 226-230, 1988.

[20] E. Arvas, M. Ross, and Y. Qian, "TE Scattering from a Conducting Cylinder of Arbitrary Cross-section Covered by Multiple Layers of Lossy Dielectrics," *IEE Proceedings H*, vol. 136, no. 6, pp. 425-430, 1989.

[21] C. A. Balanis, *Advanced Engineering Electromagnetics*, John WileySons, 1989.

Senem Makal was born in Tunceli, Turkey, in 1983. She received B.Sc. and M.Sc. degrees in Electronics and Communications Engineering from Yildiz Technical University in 2005 and 2007. She is a research assistant in the Department of Electronics and Communications Engineering at Yildiz Technical University. Her main research interests include electromagnetic wave theory, electromagnetic scattering, artificial neural networks, and radar target identification.

Ahmet Kizilay was born in Istanbul, Turkey, in 1969. He received B.Sc. degree in Electronics and Communications Engineering from Yildiz University in 1990, M.Sc. and Ph.D. degrees in Electrical Engineering from Michigan State University in 1994 and 2000. In July 2001, he joined the Department of Electronics and Communications Engineering at Yildiz Technical University, where he is currently working as Associate Professor. His main research interests include time domain electromagnetic scattering, electromagnetic wave theory, and fiber optics.